IEEE Access
Multidisciplinary | Rapid Review | Open Access Journal

Received December 16, 2019, accepted January 1, 2020, date of publication January 8, 2020, date of current version January 16, 2020.

Digital Object Identifier 10.1109/ACCESS.2020.2964823

Hue-Correction Scheme Based on Constant-Hue Plane for Deep-Learning-Based Color-Image Enhancement

YUMA KINOSHITA, (Student Member, IEEE), AND HITOSHI KIYA, (Fellow, IEEE)
Department of Computer Science, Tokyo Metropolitan University, Tokyo 191-0065, Japan

Corresponding author: Hitoshi Kiya (kiya@tmu.ac.jp)

This work was supported by Japan Society for the Promotion of Science (JSPS) Grant-in-Aid for JSPS Fellows under JSPS KAKENHI Grant Number JP18J20326.

ABSTRACT In this paper, we propose a novel hue-correction scheme based on the constant-hue plane in the RGB color space for deep-learning-based color-image enhancement. Existing hue-preserving image-enhancement methods cannot be applied to state-of-the-art enhancement methods such as deep-learning-based ones. Our main contributions are a discussion on the enhancement performance and the hue distortion of existing image-enhancement methods as well as the first attempt to make hue correction applicable to any existing image-enhancement methods including deep-learning-based ones. This novel scheme is carried out on the basis of the constant-hue plane in the RGB color space. In simulations, we first evaluated conventional image-enhancement methods in terms of the enhancement performance and hue distortion by using five objective metrics: the maximally saturated color similarity, the hue difference in CIEDE2000, discrete entropy, HIGRADE, and NIQMC. The experimental results show that recent deep-learning-based methods have a higher enhancement performance but cause images to be hue-distorted. In addition, the proposed scheme is demonstrated to be effective for suppressing hue distortion even under the use of deep-learning-based enhancement methods. Furthermore, it allows us not only to correct hue but also to maintain the performance of image-enhancement methods.

INDEX TERMS Color image enhancement, hue-preserving image enhancement, constant-hue plane, RGB color space.

I. INTRODUCTION

Single-image enhancement is one of the most typical image processing techniques. The purpose of enhancing images is to show hidden details in unclear low-quality images. Early attempts of single-image enhancement such as histogram equalization (HE) [1]–[5] focused on enhancing the contrast of grayscale images. Hence, these methods do not directly enhance color images. A way to handle color images with these methods is enhancing the luminance components of color images and then multiplying each RGB component by the ratio of enhanced and input luminance components. Although simple and efficient, methods for grayscale images have limited performance in enhancing color images. Due to this, interest in color-image enhancement, such as 3-D histogram-, Retinex-, and fusion-based enhancement, has increased [6]–[12]. In addition, recent single-image enhancement methods utilize deep neural networks trained to regress from unclear low-quality images to clear high-quality ones [13]–[19]. These deep-learning-based approaches significantly improve the performance of image enhancement compared with conventional analytical approaches such as HE. However, these color-image enhancement methods cause colors to be distorted.

To avoid color distortion, hue-preserving image-enhancement methods have also been studied [20]–[23]. Naik et al. showed conditions for preserving hue without color gamut problems. In accordance with the conditions, they proposed a hue-preserving contrast-enhancement method that uses scaling and sifting parameters in the RGB color space. However, these hue-preserving image-enhancement methods cannot be applied to state-of-the-art

The associate editor coordinating the review of this manuscript and approving it for publication was Ke Gu.

enhancement algorithms such as deep-learning-based ones since they are designed for specific enhancement algorithms. Therefore, the enhancement performance of conventional hue-preserving enhancement methods is lower than that of the state-of-the-art color-image enhancement ones.

Our main contributions in this paper are a discussion on the enhancement performance and hue distortion of existing image-enhancement methods and the first attempt to make hue correction applicable to any existing image-enhancement method including deep-learning-based ones. To develop such a hue-correction method, we first generalize a hue-preserving method [22], which is based on the constant-hue plane in the RGB color space, to any image-enhancement method. This generalization derives our novel hue-correction scheme for color-image enhancement. The proposed scheme can remove hue distortion caused by any image processing method including deep-learning-based ones by replacing the maximally saturated colors on the constant-hue planes of the enhanced image with those of the input image. In addition, the hue-correction scheme can be carried out without color gamut problems.

We evaluated image-enhancement methods in terms of hue distortion and the quality of enhanced images in a number of simulations. In the simulations, five objective metrics, the maximally saturated color similarity, the hue difference in CIEDE2000, discrete entropy, HIGRADE, and NIQMC, were utilized for the evaluation. The experimental results show that recent deep-learning-based methods have a higher enhancement performance but cause images to be hue-distorted. In addition, it is then demonstrated that the proposed scheme can correct hue distortion caused by image-enhancement methods even when deep-learning-based enhancement methods are used for enhancing images. Furthermore, it is also confirmed that the proposed scheme can maintain the performance of image-enhancement methods.

The rest of this paper is organized as follows. In Section 2, we review related work. In Section 3, we present our hue-correction scheme for deep-learning-based color-image enhancement. In Section 4, we demonstrate the hue distortion caused by image-enhancement methods and evaluate the effectiveness of the proposed hue-correction scheme. In Section 5, we conclude our study.

II. RELATED WORK

Here, we summarize typical single-image enhancement methods, including recent fusion-based ones and deep-learning-based ones, and problems with them.

A. IMAGE ENHANCEMENT

Various kinds of research on single-image enhancement have so far been reported [1]–[19], [24]–[26]. Classic enhancement methods such as histogram equalization (HE) focus on enhancing the contrast of grayscale images. For this reason, these methods do not directly handle color images. A way to handle color images with these methods is enhancing the luminance components of color images and then multiplying each RGB component by the ratio of enhanced and input luminance components. Although simple and efficient, the methods for grayscale images are limited in their ability to improve color-image quality. Due to this, interest in color-image enhancement, such as 3-D histogram-, Retinex-, and fusion-based enhancement, has increased. Today, many single-image enhancement methods utilize deep neural networks trained to regress from unclear low-quality images to clear high-quality ones.

Most classic enhancement methods were designed for grayscale images. Among these methods, histogram equalization (HE) has received the most attention because of its intuitive implementation quality and high efficiency. It aims to derive a mapping function such that the entropy of a distribution of output luminance values can be maximized. Since HE often causes over/under-enhancement problems, a huge number of HE-based methods have been developed to improve the performance of HE [1]–[5]. However, these methods cannot directly handle color images. The most common way to handle color images with these methods is enhancing the luminance components of color images and then multiplying each RGB component by the ratio of enhanced and input luminance components. Otherwise, these simple and efficient methods for grayscale images are limited in their ability to improve color-image quality. As a result, enhancement methods that can directly work on color images have been developed.

A traditional approach for enhancing color images is 3-D HE, which is an extension of normal HE [6]–[8]. In this approach, an image is enhanced so that a 3-dimensional histogram defined on RGB color space is uniformly distributed. Another way for enhancing color images is to use Retinex theory [27]. In Retinex theory, the dominant assumption is that a (color) image can be decomposed into two factors, say reflectance and illumination. Early attempts based on Retinex, such as single-scale Retinex (SSR) [24] and multi-scale Retinex (MSR) [25], treat reflectance as the final result of enhancement, yet the image often looks unnatural and frequently appears to be over-enhanced. For this reason, recent Retinex-based methods [9], [10], [26] decompose images into reflectance and illumination and then enhance images by manipulating illumination. Additionally, multi-exposure-fusion (MEF)-based single-image enhancement methods were recently proposed [11], [12], [28]. One of them, a pseudo MEF scheme [12], makes any single image applicable to MEF methods by generating pseudo multi-exposure images from a single image. By using this scheme, images with improved quality are produced with the use of detailed local features. Furthermore, quality-optimized image enhancement algorithms [29]–[31] enable us to automatically set parameters in these algorithms and enhance images, by finding optimal parameters in terms of a no-reference image quality metric. Recent work has demonstrated great progress by using data-driven approaches in preference to analytical approaches such as HE [13]–[19].

These data-driven approaches utilize pairs of high- and low-quality images to train deep neural networks, and the trained networks can be used to enhance color images.

The approaches can directly enhance color images, but the resulting colors are distorted.

B. HUE-PRESERVING IMAGE ENHANCEMENT

Hue-preserving image-enhancement methods have also been studied to avoid color distortion [20]–[23]. Naik et al. showed conditions for preserving hue without color gamut problems. In accordance with the conditions, they proposed a hue-preserving contrast-enhancement method that uses scaling and sifting parameters in the RGB color space [20]. Although their method can enhance the contrast while keeping the hue, the resulting colors will often have low chroma. To overcome the problem, Nikolova et al. improved Naik's method in terms of chromaticness by using a histogram specification algorithm [21]. Ueda et al. also proposed a hue-preserving enhancement method that is an extended version of Naik's method [22]. Ueda's method enables us to enhance not only brightness components but also chroma components in the manner of HE.

However, these methods cannot be applied to state-of-the-art methods for color-image enhancement such as deep-learning-based ones since they were designed for specific enhancement algorithms. Hence, the enhancement performance of hue-preserving methods is limited compared with these color-image enhancement methods. In addition to image enhancement, hue-preserving image-processing methods have been studied in other research areas such as image denoising [32], but they are similarly designed for specific algorithms. For this reason, we propose a novel hue-preserving image-enhancement scheme that is applicable to any existing image-enhancement method including deep-learning-based ones.

III. PROPOSED HUE-CORRECTION SCHEME

Figure 1 shows the difference between conventional hue-preserving image-enhancement methods and our hue-correction scheme for color-image enhancement. As shown in Fig. 1(a), conventional methods enhance images by using specific algorithms that preserve the hue components of input images. The use of a specific algorithm for enhancement prevents us from applying hue-preserving enhancement to the state-of-the-art enhancement algorithms. For this reason, we discuss the first attempt to develop a hue-correction scheme that is applicable to any image-enhancement method including deep-learning-based ones [see Fig. 1(b)].

In the proposed scheme, we first enhance an input image I by using a state-of-the-art image-enhancement method such as Retinex- and deep-learning-based ones. This enhancement will cause hue distortion in the enhanced image $\hat{I}$. For this reason, hue correction, which is based on the constant-hue plane in the RGB color space [22], is then carried out in order to remove the distortion. Hue correction enables us not only to match hue components before and after the enhancement but also to maintain the performance of image enhancement.

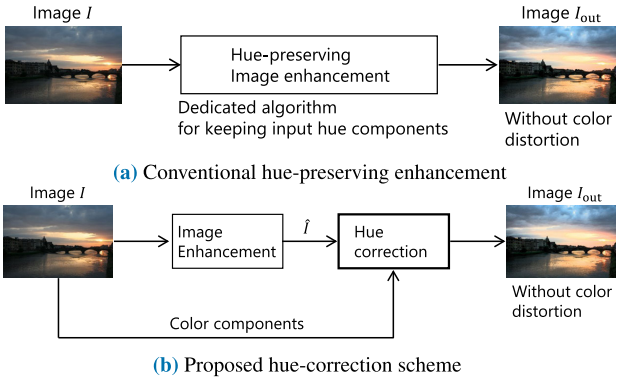

FIGURE 1. Proposed hue-correction scheme. Proposed scheme is first attempt to make hue correction applicable to any image-enhancement method. In proposed scheme, hue distortion caused by enhancement is removed by using color components of input image. In contrast, conventional methods use dedicated enhancement algorithm to enhance image while keeping hue of input image.

A. NOTATION

The following notations are used throughout this paper.

- Lower case bold italic letters, e.g., $\boldsymbol{x}$, denote column vectors and are used only for denoting coordinates in the RGB color space.
- The superscript $\top$ denotes the transpose of a matrix or vector.
- The notation $(x_1, x_2, \ldots, x_N)$ denotes an N-dimensional row vector.
- An RGB color pixel value is denoted by a 3-dimensional column vector, where first, second, and third elements indicate red, green, and blue components, respectively. For example, an RGB pixel value $\boldsymbol{x}$ can be written as $\boldsymbol{x} = (x_r, x_g, x_b)^\top$.
- I is used to denote an image and is a set of all pixel values.

B. CONSTANT-HUE PLANE

Each pixel value of an RGB color image can be represented as $\boldsymbol{x} \in [0, 1]^3$, where the R, G, and B components of the pixel value $\boldsymbol{x}$ are written as x_r, x_g, and x_b, respectively. In the RGB color space, a set of pixels that have the same hue forms a plane [22], called a "constant-hue plane," as shown in Fig. 2. Here, the expression of hue considered in this paper is the hue as defined in HSI color space [20]. The shape of each constant-hue plane is a triangle whose vertices correspond to white $\boldsymbol{w} = (1, 1, 1)^\top$, black $\boldsymbol{k} = (0, 0, 0)^\top$, and a maximally saturated color $\boldsymbol{c}$ [22], [33]. The maximally saturated color $\boldsymbol{c} = (c_r, c_g, c_b)^\top$, which has the same hue as that of $\boldsymbol{x}$, is calculated by

$$\begin{aligned} c_r &= \frac{x_r - \min(\boldsymbol{x})}{\max(\boldsymbol{x}) - \min(\boldsymbol{x})}, \\ c_g &= \frac{x_g - \min(\boldsymbol{x})}{\max(\boldsymbol{x}) - \min(\boldsymbol{x})}, \\ c_b &= \frac{x_b - \min(\boldsymbol{x})}{\max(\boldsymbol{x}) - \min(\boldsymbol{x})}, \end{aligned} \tag{1}$$

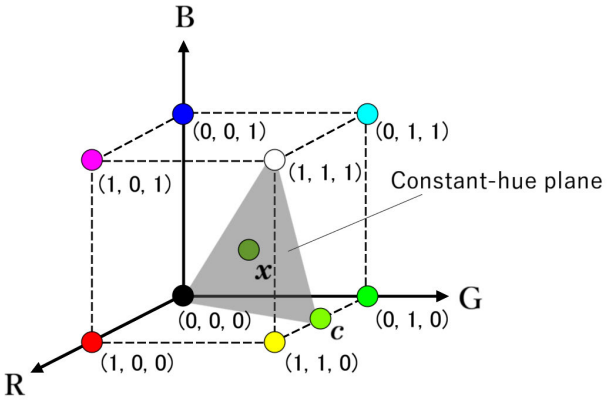

FIGURE 2. Conceptual diagram of RGB color space. Gray triangle denotes constant-hue plane for pixel value x.

where $\max(\cdot)$ and $\min(\cdot)$ are functions that return the maximum and minimum elements of the pixel value $\boldsymbol{x}$, respectively.

On the constant-hue plane, the pixel value $\boldsymbol{x}$ can be represented as a linear combination with

$$\boldsymbol{x} = a_w \boldsymbol{w} + a_k \boldsymbol{k} + a_c \boldsymbol{c}, \tag{2}$$

where

$$\begin{aligned} a_w &= \min(\boldsymbol{x}), \\ a_c &= \max(\boldsymbol{x}) - \min(\boldsymbol{x}), \\ a_k &= 1 - \max(\boldsymbol{x}). \end{aligned} \tag{3}$$

Since $\boldsymbol{x}$ is an interior point on the plane spanned by $\boldsymbol{w}, \boldsymbol{k}$, and $\boldsymbol{c}$, the following equations hold

$$a_w + a_k + a_c = 1, \tag{4}$$

$$0 \leq a_w, a_k, a_c \leq 1. \tag{5}$$

C. DERIVING PROPOSED HUE CORRECTION

Ueda et al. proposed a hue-preserving image-enhancement method based on the constant-hue plane [22]. They realized hue-preserving enhancement by manipulating coefficients a_w, a_k, and a_c, not RGB values. However, Ueda's method cannot be applied to conventional color-image-enhancement methods including Retinex- and deep-learning-based ones since conventional enhancement methods are not designed for enhancing a_w, a_k, and a_c. In this section, we derive a novel hue-correction scheme that is applicable to any existing image enhancement method on the basis of the constant-hue plane.

In Ueda's method [22], the maximum saturated color $\boldsymbol{c}$ and coefficients a_w, a_k, and a_c are first calculated from each pixel value $\boldsymbol{x}$ by using eqs. (1) and (3), respectively. Coefficients a_w, a_k, and a_c are then independently enhanced by an HE-based algorithm:

$$\begin{aligned} a'_w &= G^{-1}_{w,\sigma_w}(F_w(a_w)), \\ a'_k &= G^{-1}_{k,\sigma_k}(F_k(a_k)), \\ a'_c &= G^{-1}_{c,\sigma_c}(F_c(a_c)), \end{aligned} \tag{6}$$

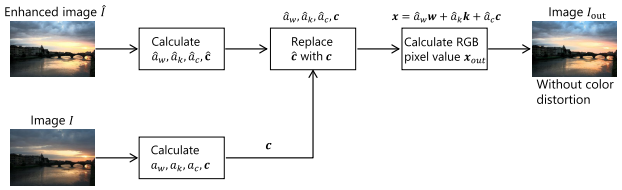

FIGURE 3. Hue-correction procedure.

where F_w, F_k, and F_c denote cumulative distribution functions of a_w, a_k, and a_c, respectively. Also, $G^{-1}_{w,\sigma_w}, G^{-1}_{k,\sigma_k}$, and G^{-1}_{c,σ_c} indicate the inverse of the smoothed cumulative distribution functions of a_w, a_k, and a_c, respectively. This enhancement does not cause any hue distortion since the constant-hue plane spanned by $\boldsymbol{w}, \boldsymbol{k}$, and $\boldsymbol{c}$ is unchanged through this enhancement.

Because general color-image-enhancement methods do not preserve $\boldsymbol{c}$, they cause enhanced images to be hue-distorted. Therefore, we aim to remove hue distortion due to enhancement by using the constant-hue plane. In our hue-correction scheme, the hue information of an input image is utilized to remove hue distortion in the corresponding enhanced image.

D. PROPOSED PROCEDURE

The procedure of our hue-correction scheme is shown as follows (see also Fig.3).

1) Obtain an enhanced image $\hat{I}$ by applying an image-enhancement method f to input image I as

$$\hat{I} = f(I). \tag{7}$$

2) Calculate the maximum saturated color $\boldsymbol{c}$ and coefficients a_w, a_k, and a_c from each pixel value $\boldsymbol{x}$ in I by using eqs. (1) and (3), respectively.
3) Calculate the maximum saturated color $\hat{\boldsymbol{c}}$ and coefficients $\hat{a}_w, \hat{a}_k$, and $\hat{a}_c$ from each pixel value $\hat{\boldsymbol{x}}$ in $\hat{I}$ by using eqs. (1) and (3), respectively, and obtain

$$\hat{\boldsymbol{x}} = \hat{a}_w \boldsymbol{w} + \hat{a}_k \boldsymbol{k} + \hat{a}_c \hat{\boldsymbol{c}}. \tag{8}$$

4) Replace $\hat{\boldsymbol{c}}$ with $\boldsymbol{c}$, and obtain

$$\boldsymbol{x}_{out} = \hat{a}_w \boldsymbol{w} + \hat{a}_k \boldsymbol{k} + \hat{a}_c \boldsymbol{c}. \tag{9}$$

5) Calculate each output RGB pixel value $\boldsymbol{x}_{out} = (x_{out_r}, x_{out_g}, x_{out_b})^\top$ in accordance with eq. (2), as

$$\begin{aligned} x_{out_r} &= \hat{a}_w + \hat{a}_c c_r, \\ x_{out_g} &= \hat{a}_w + \hat{a}_c c_g, \\ x_{out_b} &= \hat{a}_w + \hat{a}_c c_b. \end{aligned} \tag{10}$$

6) Obtain output image I_{out} that has $\boldsymbol{x}_{out}$ as pixel values.

Here, replacing $\hat{\boldsymbol{c}}$ with $\boldsymbol{c}$ in Step 4 corresponds to correcting hue in the HSI color space. In addition, since a_w, a_k, and a_c satisfy eqs. (4) and (5), the replacement can be performed without gamut problems in contrast to directly replacing hue in the HSI color space.

In contrast, the proposed scheme has a limitation: once colored pixels become gray values by an enhancement method (i.e., $\hat{x}_r = \hat{x}_g = \hat{x}_b$), the proposed scheme cannot correct these colors, because $\hat{a}_c = 0$ is given under $\hat{x}_r = \hat{x}_g = \hat{x}_b$ from eq. (3), so the equation

$$\begin{aligned}\hat{\boldsymbol{x}} &= \hat{a}_w \boldsymbol{w} + \hat{a}_k \boldsymbol{k} + \hat{a}_c \hat{\boldsymbol{c}} \\ &= \hat{a}_w \boldsymbol{w} + \hat{a}_k \boldsymbol{k} + \hat{a}_c \boldsymbol{c} \\ &= \boldsymbol{x}_{out}\end{aligned} \tag{11}$$

is satisfied for these pixels. However, even when some colored pixels become gray values, other pixels can be corrected by using the proposed scheme. Therefore, the proposed scheme is valid even under this limitation.

For these reasons, the proposed scheme enables us not only to remove hue distortion but also to ensure that all pixel values after hue correction are included in the RGB color gamut.

IV. SIMULATION

We evaluated the effectiveness of the proposed scheme by using five objective metrics including two color difference formulae.

A. ENHANCEMENT PERFORMANCE

We first confirmed the performance of image-enhancement methods without any hue-preserving or hue-correction operations in a simulation. Seven methods were evaluated: HE, contrast-accumulated HE (CACHE) [5], simultaneous reflectance and illumination estimation (SRIE) [9], low-light image enhancement via illumination map estimation (LIME) [10], pseudo multi-exposure image fusion (PMEF) [12], iTM-Net [34], and deep underexposed photo enhancement (deepUPE) [18]. Here, HE and CACHE are HE-based methods, SRIE and LIME are Retinex-based ones, PMEF is an MEF-based one, and iTM-Net and deepUPE are deep-learning-based ones. Eight input images selected from the EasyHDR dataset [35] were used for the simulation.

The performance of the enhancement methods was evaluated by using three objective image quality metrics: discrete entropy, the HDR image gradient based evaluator (HIGRADE) [36], and one of no-reference image quality metrics for contrast distortion (NIQMC) [37]. Discrete entropy represents the amount of information in an image. HIGRADE represents the quality of an image tone-mapped from a high dynamic range (HDR) image; the evaluator calculates quality scores of images without any reference images. Since the process of photographing is similar to tone mapping, HIGRADE is also useful for evaluating photographs. NIQMC assesses the quality of contrast-distorted images by considering both local and global information [37].

Tables 1, 2, and 3 show scores for discrete entropy, HIGRADE and NIQMC, respectively. For each score, a larger value means higher quality. As shown in Tables 1, 2, and 3, recent image-enhancement methods such as LIME and deepUPE produced better images than traditional HE-based ones in terms of entropy and HIGRADE, while HE-based ones provided high scores for NIQMC. Figure 4 illustrates an example of enhanced images. By comparing enhanced images shown in Fig. 4, it is also confirmed that the recent enhancement methods, i.e., LIME and deepUPE, generated more clear images than traditional HE-based ones. Hence, using the state-of-the-art methods is required to obtain high-quality enhanced images.

TABLE 1. Performance of conventional enhancement methods (Entropy). Recent enhancement methods such as LIME and deepUPE have higher performance than traditional HE.

Scene	HE	CACHE	SRIE	LIME	PMEF	iTM-Net	deepUPE
Arno	6.880	7.450	7.188	**7.659**	6.871	6.561	7.544
Chinese Garden	6.669	7.111	6.458	**7.310**	6.762	6.768	7.064
Estate rsa	6.941	**7.564**	6.821	7.532	6.579	6.389	7.234
Kluki	6.276	7.633	7.592	7.359	7.331	6.878	**7.706**
Laurenziana	6.399	7.189	7.296	**7.546**	7.101	6.792	7.468
Mountains	6.018	**7.901**	7.352	7.336	7.186	5.636	7.519
Ostrow Tumski	6.758	7.451	7.183	**7.595**	7.319	6.855	7.227
Average	6.563	7.471	7.127	**7.477**	7.022	6.554	7.395

TABLE 2. Performance of conventional enhancement methods (HIGRADE). Recent enhancement methods such as LIME and deepUPE have higher performance than traditional HE.

Scene	HE	CACHE	SRIE	LIME	PMEF	iTM-Net	deepUPE
Arno	0.439	0.557	0.690	**0.749**	0.382	0.277	0.678
Chinese garden	0.380	**0.447**	0.282	0.247	0.294	0.250	0.418
Estate rsa	0.372	**0.372**	0.124	0.299	0.220	-0.105	0.331
Kluki	0.472	0.539	0.512	**0.721**	0.522	0.271	0.462
Laurenziana	-0.205	**0.617**	0.262	0.386	0.194	-0.012	0.228
Mountains	0.132	0.529	0.538	0.588	**0.687**	-0.247	0.523
Ostrow tumski	-0.021	0.311	0.517	**0.560**	-0.017	0.379	0.392
Average	0.224	0.482	0.418	**0.507**	0.326	0.116	0.433

TABLE 3. Performance of conventional enhancement methods (NIQMC). Recent enhancement methods such as LIME and deepUPE have higher performance than traditional HE.

Scene	HE	CACHE	SRIE	LIME	PMEF	iTM-Net	deepUPE
Arno	5.799	**5.823**	5.416	5.437	5.478	4.682	5.543
Chinese garden	5.842	**5.847**	5.167	5.542	5.496	4.793	5.554
Estate rsa	**5.830**	5.827	4.832	5.029	5.003	4.066	5.159
Kluki	5.656	**5.776**	5.787	5.478	5.604	4.870	5.609
Laurenziana	**5.753**	5.729	5.633	5.527	5.488	4.801	5.719
Mountains	5.562	**5.643**	4.765	4.548	5.104	3.346	5.054
Ostrow tumski	5.752	**5.805**	5.478	5.560	5.138	5.035	5.321
Average	5.742	**5.779**	5.297	5.303	5.330	4.513	5.423

B. HUE DISTORTION

We also evaluated the hue distortion caused by the enhancement methods without any hue-preserving or hue-correction operations. Hue distortion after enhancement was measured by using the cosine similarity between input maximally

(a) Input (b) HE (c) CACHE

(d) SRIE (e) LIME (f) PMEF

(g) iTM-Net (h) deepUPE

FIGURE 4. Results of image enhancement (for image "Arno") .

TABLE 4. Hue distortion due to enhancement (cosine similarity between maximally saturated colors). Enhancement methods, such as HE, CACHE, and SRIE, which enhance only luminance components, cause less distortion than recent color-image enhancement methods.

Scene	HE	CACHE	SRIE	LIME	PMEF	iTM-Net	deepUPE
Arno	0.984	0.999	**1.000**	0.998	0.948	0.945	0.929
Chinese garden	0.987	0.997	**1.000**	0.938	0.911	0.918	0.947
Estate rsa	0.982	0.996	**1.000**	0.975	0.986	0.949	0.976
Kluki	0.986	**1.000**	**1.000**	0.939	0.938	0.863	0.954
Laurenziana	0.987	0.997	**1.000**	0.957	0.923	0.907	0.966
Mountains	0.984	0.999	**1.000**	0.984	1.000	0.977	0.987
Ostrow tumski	0.999	0.999	**1.000**	0.997	0.913	0.891	0.875
Average	0.987	0.998	**1.000**	0.970	0.946	0.921	0.948

TABLE 5. Hue distortion due to enhancement (hue difference $\Delta H'$). Enhancement methods, such as HE, CACHE, and SRIE, which enhance only luminance components, cause less distortion than recent color-image enhancement methods.

Scene	HE	CACHE	SRIE	LIME	PMEF	iTM-Net	deepUPE
Arno	1.375	1.103	**0.014**	0.644	2.612	1.384	3.619
Chinese garden	0.313	0.737	**0.173**	0.708	0.646	1.406	2.689
Estate rsa	0.728	1.693	**0.030**	0.339	0.556	1.252	2.220
Kluki	**0.010**	0.214	0.175	0.509	1.395	1.455	3.636
Laurenziana	0.094	0.631	**0.080**	0.544	0.563	1.412	1.821
Mountains	0.081	0.395	**0.000**	0.036	0.222	1.354	1.068
Ostrow tumski	0.669	0.699	**0.024**	0.425	5.733	1.288	3.067
Average	0.467	0.782	**0.071**	0.458	1.675	1.364	2.589

saturated colors $\boldsymbol{c}$ and output ones $\boldsymbol{c}_{out}$ and the hue difference $\Delta H'$ of the CIEDE2000 [38], where corresponding input images were utilized as reference images for calculating $\Delta H'$.

Tables 4 and 5 show the scores for the cosine similarity and the hue difference $\Delta H'$. The scores were calculated as the absolute average of the cosine similarity and $\Delta H'$ for all pixels, respectively. For the similarity $\in [0, 1]$, a larger value means higher hue-similarity. In contrast, a lower value means less of a hue difference for the $\Delta H'$. From the tables, it was confirmed that LIME, PMEF, and the two deep-learning-based methods caused large hue distortion compared with HE, CACHE, and SRIE, although LIME and deepUPE had a higher-enhancement performance. This is because recent enhancement methods such as LIME directly enhance RGB color components, not luminance components.

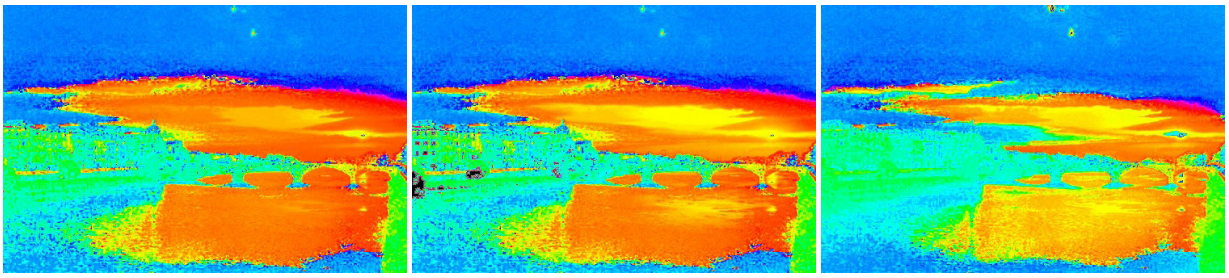

(a) Input (b) HE (c) deepUPE

FIGURE 5. Maximally saturated colors of enhanced images (for image "Arno").

TABLE 6. Cosine similarity between maximally saturated colors for conventional hue-preserving image-enhancement methods and proposed hue-correction scheme (for EasyHDR dataset [35]). Numbers in parentheses denote score of each corresponding enhancement method without proposed scheme. Use of proposed scheme enabled us to suppress hue distortion caused by any of image-enhancement methods.

Scene	Naik	Ueda	With Proposed (without proposed)			
			LIME	PMEF	iTM-Net	deepUPE
Arno	**1.000**	**1.000**	0.999 (0.998)	0.958 (0.948)	**1.000** (0.945)	0.999 (0.929)
Chinese garden	**1.000**	**1.000**	0.939 (0.938)	0.918 (0.911)	**1.000** (0.918)	**1.000** (0.947)
Estate rsa	**1.000**	**1.000**	0.976 (0.975)	0.986 (0.986)	**1.000** (0.949)	**1.000** (0.976)
Kluki	**1.000**	**1.000**	0.940 (0.939)	0.960 (0.938)	**1.000** (0.863)	**1.000** (0.954)
Laurenziana	**1.000**	**1.000**	0.960 (0.957)	0.927 (0.923)	**1.000** (0.907)	**1.000** (0.966)
Mountains	**1.000**	**1.000**	0.984 (0.984)	**1.000** (1.000)	**1.000** (0.977)	0.999 (0.987)
Ostrow tumski	**1.000**	**1.000**	0.998 (0.997)	0.943 (0.913)	**1.000** (0.891)	0.999 (0.875)
Average	**1.000**	**1.000**	0.971 (0.970)	0.956 (0.946)	**1.000** (0.921)	0.999 (0.948)

TABLE 7. Hue difference $\Delta H'$ between input and enhanced images (for EasyHDR dataset [35]). Numbers in parentheses denote score of each corresponding enhancement method without proposed scheme. Use of proposed scheme enabled us to suppress hue distortion caused by any of image-enhancement methods.

Scene	Naik	Ueda	With Proposed (without proposed)			
			LIME	PMEF	iTM-Net	deepUPE
Arno	0.144	0.726	**0.051** (0.644)	1.338 (2.612)	0.201 (1.384)	0.249 (3.619)
Chinese garden	0.355	0.719	0.398 (0.708)	0.455 (0.646)	**0.354** (1.406)	0.383 (2.689)
Estate rsa	0.441	0.607	**0.049** (0.339)	0.553 (0.556)	0.362 (1.252)	0.217 (2.220)
Kluki	0.476	0.590	**0.305** (0.509)	1.016 (1.395)	0.669 (1.455)	0.403 (3.636)
Laurenziana	0.200	0.609	**0.189** (0.544)	0.416 (0.563)	0.220 (1.412)	0.194 (1.821)
Mountains	0.006	1.375	**0.002** (0.036)	0.222 (0.222)	0.150 (1.354)	0.058 (1.068)
Ostrow tumski	0.082	0.786	**0.079** (0.425)	2.523 (5.733)	0.215 (1.288)	0.229 (3.067)
Average	0.243	0.773	**0.153** (0.458)	0.932 (1.675)	0.310 (1.364)	0.248 (2.589)

Figure 5 shows maximally saturated colors of an input image and two enhanced images. This figure also illustrates that deepUPE significantly changed the maximally saturated colors, but HE preserved them.

In the next section, we apply the proposed scheme to the four methods that lead to large hue distortion to remove the distortion.

C. HUE CORRECTION RESULTS

To confirm that the proposed scheme is applicable to various color-image enhancement methods, we applied it to four such methods: LIME, PMEF, iTM-Net, and deepUPE. The performance of the proposed scheme was compared with two conventional hue-preserving image-enhancement methods: Naik's method [20] and Ueda's method [22]. In addition to the 8 images in the dataset [35], 500 images selected from the MIT-Adobe FiveK dataset [39] were used for the simulation, where the 500 images were the same as test images that were used in [18].

The hue distortion after applying the proposed scheme is shown in Tables 6 and 7. Comparing Tables 4 and 6 (or Tables 5 and 7), the use of the proposed method suppressed

(a) Naik [20] (b) Ueda [22] (c) LIME with proposed scheme

(d) PMEF with proposed scheme (e) iTM-Net with proposed scheme (f) deepUPE with proposed scheme

FIGURE 6. Results of hue correction (for image "Arno") .

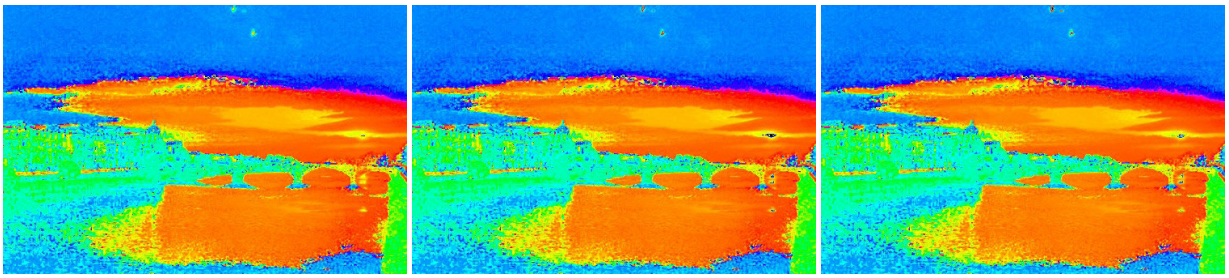

(a) Ueda [22] (b) LIME with proposed scheme (c) deepUPE with proposed scheme

FIGURE 7. Maximally saturated colors of hue corrected images (for image "Arno").

TABLE 8. Entropy scores (for EasyHDR dataset [35]). Use of proposed scheme enabled us to preserve performance of image-enhancement methods.

Scene	Naik	Ueda	Proposed			
			LIME	PMEF	iTM-Net	deepUPE
Arno	6.844	6.955	**7.639**	6.703	6.598	7.517
Chinese garden	7.262	7.094	**7.335**	6.770	6.729	7.038
Estate rsa	6.931	6.756	**7.527**	6.578	6.383	7.193
Kluki	7.335	7.290	7.391	7.319	6.843	**7.710**
Laurenziana	7.318	7.276	**7.582**	7.106	6.714	7.458
Mountains	6.889	**7.579**	7.339	7.186	5.691	7.550
Ostrow tumski	6.869	7.211	**7.586**	7.071	6.922	7.244
Average	7.064	7.166	**7.485**	6.962	6.554	7.387

TABLE 9. HIGRADE scores (for EasyHDR dataset [35]). Use of proposed scheme enabled us to preserve performance of image-enhancement methods.

Scene	Naik	Ueda	Proposed			
			LIME	PMEF	iTM-Net	deepUPE
Arno	0.372	0.293	**0.707**	0.310	0.369	0.557
Chinese garden	-0.037	0.174	0.242	0.274	0.322	**0.331**
Estate rsa	0.237	0.160	**0.304**	0.195	-0.004	0.271
Kluki	0.471	0.350	**0.672**	0.506	0.262	0.513
Laurenziana	0.036	-0.118	**0.377**	0.181	0.001	0.234
Mountains	0.086	0.533	0.602	**0.687**	-0.133	0.615
Ostrow tumski	-0.099	-0.160	**0.496**	-0.278	0.438	0.377
Average	0.152	0.176	**0.486**	0.268	0.179	0.414

the hue distortion for all four enhancement methods, in terms of both the cosine similarity and the hue difference $\Delta H'$. In the case of LIME and PMEF with the proposed scheme, most cosine similarities between maximally saturated colors were not 1, even though the proposed scheme replaced the maximally saturated colors of the enhanced images with those of the input images. This is because enhancement methods including LIME and PMEF often map colored pixels onto

TABLE 10. NIQMC scores (for EasyHDR dataset [35]). Use of proposed scheme enabled us to preserve performance of image-enhancement methods.

Scene	Naik	Ueda	Proposed			
			LIME	PMEF	iTM-Net	deepUPE
Arno	**5.687**	5.456	5.379	5.313	4.778	5.557
Chinese garden	**5.762**	5.537	5.553	5.504	4.754	5.554
Estate rsa	**5.581**	5.280	5.022	4.998	4.057	5.138
Kluki	**5.875**	5.453	5.507	5.584	4.819	5.637
Laurenziana	**5.745**	5.595	5.543	5.490	4.785	5.722
Mountains	5.606	**5.721**	4.527	5.109	3.306	5.088
Ostrow tumski	**5.636**	5.584	5.545	5.147	5.170	5.369
Average	**5.699**	5.518	5.297	5.306	4.524	5.438

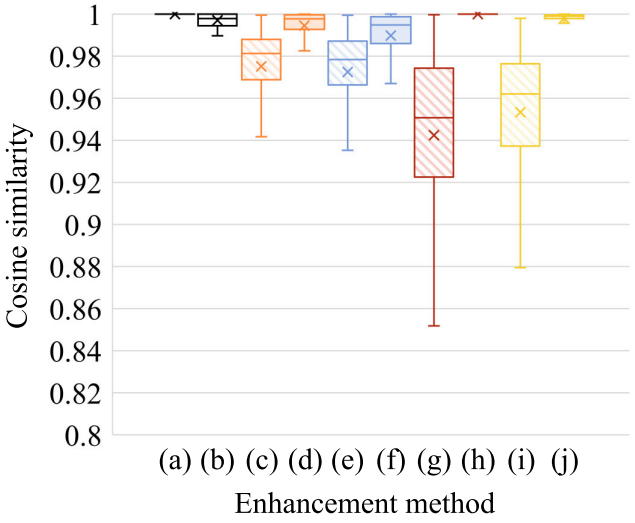

FIGURE 8. Cosine similarity between maximally saturated colors (for EasyHDR dataset [39]). (a) Naik's method, (b) Ueda's method, (c) LIME, (d) LIME with proposed scheme, (e) PMEF, (f) PMEF with proposed scheme, (g) iTM-Net, (h) iTM-Net with proposed scheme, (i) deepUPE, and (j) deepUPE with proposed scheme. Boxes span from first to third quartile, referred to as Q_1 and Q_3, and whiskers show maximum and minimum values in range of $[Q_1 - 1.5(Q_3 - Q_1), Q_3 + 1.5(Q_3 - Q_1)]$. Band and cross inside boxes indicate median and average value, respectively. Use of proposed scheme enabled us to suppress hue distortion caused by any of image-enhancement methods.

gray ones. Once colored pixels become gray, the proposed scheme cannot correct these colors since a_c in eq. (3) for a gray pixel is 0.

Tables 8, 9, and 10 show scores of discrete entropy, HIGRADE, and NIQMC, respectively. As shown in Tables 8, 9, and 10, the proposed scheme produced almost the same scores as the corresponding enhancement methods for the three metrics. Therefore, the proposed scheme can maintain the performance of image enhancement. This result was also confirmed from the hue-corrected images as shown in Fig. 6. Furthermore, by comparing the maximally saturated colors shown in Fig. 7 with those shown in Fig. 5, we can see that the proposed scheme removed the distortions of the maximally saturated colors and the corrected maximally saturated colors were almost the same as those of the input image.

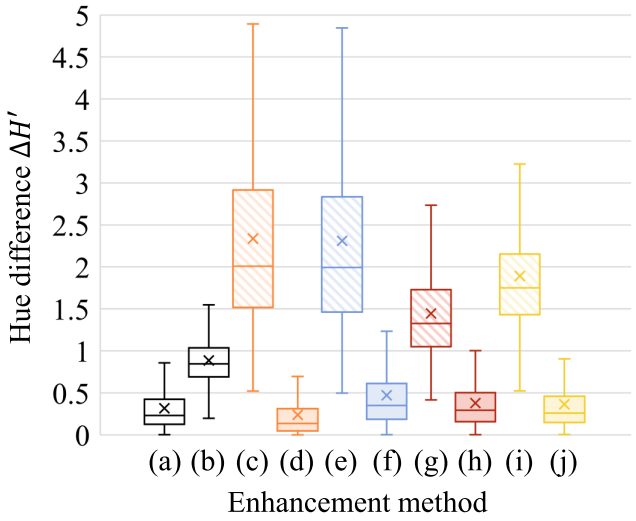

FIGURE 9. Hue difference $\Delta H'$ between input and enhanced images (for MIT-Adobe FiveK dataset [39]). (a) Naik's method, (b) Ueda's method, (c) LIME, (d) LIME with proposed scheme, (e) PMEF, (f) PMEF with proposed scheme, (g) iTM-Net, (h) iTM-Net with proposed scheme, (i) deepUPE, and (j) deepUPE with proposed scheme. Boxes span from first to third quartile, referred to as Q_1 and Q_3, and whiskers show maximum and minimum values in range of $[Q_1 - 1.5(Q_3 - Q_1), Q_3 + 1.5(Q_3 - Q_1)]$. Band and cross inside boxes indicate median and average value, respectively. Use of proposed scheme enabled us to suppress hue distortion caused by any of image-enhancement methods.

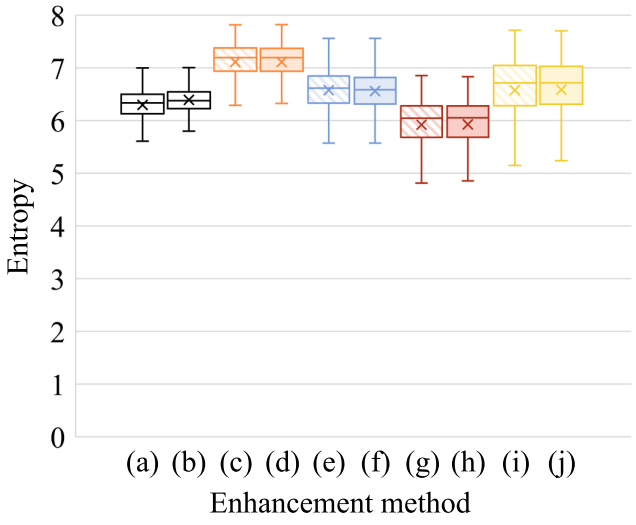

FIGURE 10. Entropy scores (for MIT-Adobe FiveK dataset [39]). (a) Naik's method, (b) Ueda's method, (c) LIME, (d) LIME with proposed scheme, (e) PMEF, (f) PMEF with proposed scheme, (g) iTM-Net, (h) iTM-Net with proposed scheme, (i) deepUPE, and (j) deepUPE with proposed scheme. Boxes span from first to third quartile, referred to as Q_1 and Q_3, and whiskers show maximum and minimum values in range of $[Q_1 - 1.5(Q_3 - Q_1), Q_3 + 1.5(Q_3 - Q_1)]$. Band and cross inside boxes indicate median and average value, respectively. Applying recent image-enhancement methods to proposed scheme provides increased performance over conventional hue-preserving image-enhancement methods.

Table 6 also shows that the two conventional hue-preserving methods provided the maximum cosine similarity for all eight images. Their enhancement performance was limited compared with the proposed scheme, as shown

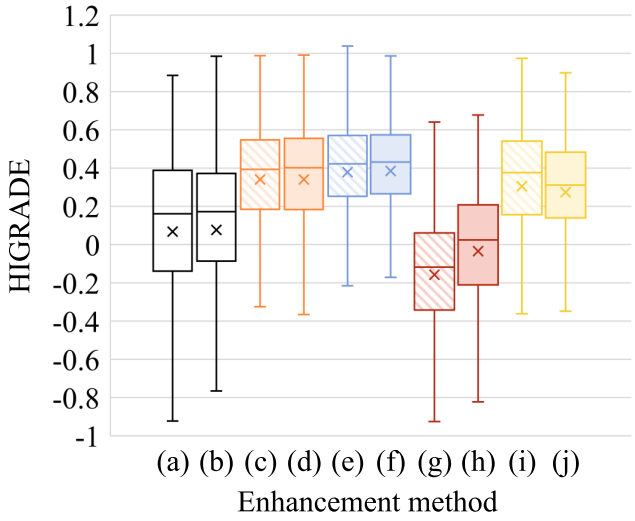

FIGURE 11. HIGRADE scores (for MIT-Adobe FiveK dataset [39]). (a) Naik's method, (b) Ueda's method, (c) LIME, (d) LIME with proposed scheme, (e) PMEF, (f) PMEF with proposed scheme, (g) iTM-Net, (h) iTM-Net with proposed scheme, (i) deepUPE, and (j) deepUPE with proposed scheme. Boxes span from first to third quartile, referred to as Q_1 and Q_3, and whiskers show maximum and minimum values in range of $[Q_1 - 1.5(Q_3 - Q_1), Q_3 + 1.5(Q_3 - Q_1)]$. Band and cross inside boxes indicate median and average value, respectively. Applying recent image-enhancement methods to proposed scheme increased performance over conventional hue-preserving image-enhancement methods.

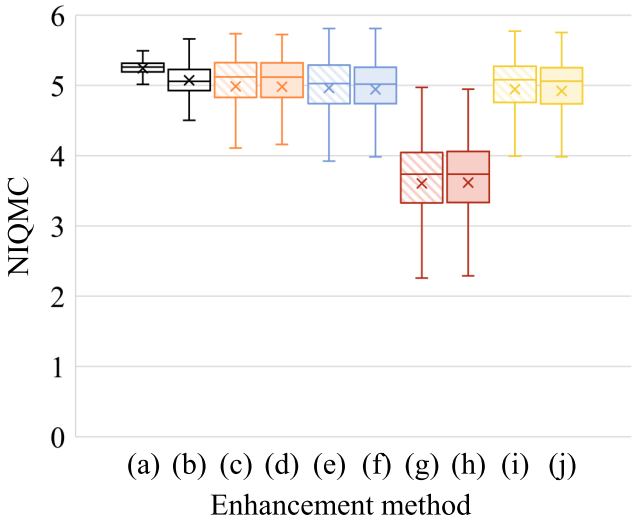

FIGURE 12. NIQMC scores (for MIT-Adobe FiveK dataset [39]). (a) Naik's method, (b) Ueda's method, (c) LIME, (d) LIME with proposed scheme, (e) PMEF, (f) PMEF with proposed scheme, (g) iTM-Net, (h) iTM-Net with proposed scheme, (i) deepUPE, and (j) deepUPE with proposed scheme. Boxes span from first to third quartile, referred to as Q_1 and Q_3, and whiskers show maximum and minimum values in range of $[Q_1 - 1.5(Q_3 - Q_1), Q_3 + 1.5(Q_3 - Q_1)]$. Band and cross inside boxes indicate median and average value, respectively.

in Tables 8 and 9. The same trend was confirmed in an experiment done using the MIT-Adobe FiveK dataset. Figures 8, 9, 10, 11, and 12 summarize quantitative evaluation results as box plots for the 500 images in the MIT-Adobe FiveK dataset in terms of the cosine similarity, the hue-difference $\Delta H'$, entropy, HIGRADE, and NIQMC, respectively. The boxes span from the first to the third quartile, referred to as Q_1 and Q_3, and the whiskers show the maximum and the minimum values in the range of $[Q_1 - 1.5(Q_3 - Q_1), Q_3 + 1.5(Q_3 - Q_1)]$. The band inside boxes indicates the median, i.e., the second quartile Q_2, and the cross inside boxes denotes the average value. Figures 8, 9, 10, 11, and 12 illustrate that the proposed scheme suppressed hue distortion as well as the conventional hue-preserving methods and maintained the performance of the image-enhancement methods. Furthermore, applying the proposed scheme to a recent enhancement method, such as LIME and deepUPE, enabled us to increase the performance of enhancement over the conventional hue-preserving ones, in terms of entropy and HIGRADE.

Therefore, the proposed scheme is effective for suppressing the hue distortion caused by image-enhancement methods including deep-learning-based ones while maintaining their performance.

V. CONCLUSION

In this paper, we proposed a novel hue-correction scheme based on the constant-hue plane in the RGB color space for color-image enhancement. To derive the proposed scheme, we generalized a hue-preserving method based on the constant-hue plane. In the proposed scheme, any existing image-enhancement method including deep-learning-based ones can be used to enhance images. Hue distortion caused by the enhancement is then removed by replacing the maximally saturated colors of an enhanced image with those of the corresponding input one. We first confirmed that recent color-image enhancement methods, i.e., LIME, PMEF, iTM-Net, and deepUPE, cause large hue distortion compared with traditional HE, CACHE, and SRIE, although LIME and deepUPE have higher-enhancement performance in terms of discrete entropy and HIGRADE, by a number of simulations. In another evaluation, experimental results showed that the proposed scheme can suppress the hue distortion caused by the four color-image enhancement methods including deep-learning-based ones, by using the cosine similarity of maximally saturated colors and the hue difference in CIEDE2000. Furthermore, objective quality evaluations demonstrated that the proposed scheme can maintain the performance of image-enhancement methods, in terms of discrete entropy, HIGRADE, and NIQMC.

REFERENCES

[1] K. Zuiderveld, "Contrast limited adaptive histogram equalization," in *Graphics Gems IV*, P. S. Heckbert, Ed. San Diego, CA, USA: Elsevier, 1994, pp. 474–485.

[2] D. Sheet, H. Garud, A. Suveer, M. Mahadevappa, and J. Chatterjee, "Brightness preserving dynamic fuzzy histogram equalization," *IEEE Trans. Consum. Electron.*, vol. 56, no. 4, pp. 2475–2480, Nov. 2010.

[3] T. Celik and T. Tjahjadi, "Automatic image equalization and contrast enhancement using gaussian mixture modeling," *IEEE Trans. Image Process.*, vol. 21, no. 1, pp. 145–156, Jan. 2012.

[4] S.-C. Huang, F.-C. Cheng, and Y.-S. Chiu, "Efficient contrast enhancement using adaptive gamma correction with weighting distribution," *IEEE Trans. Image Process.*, vol. 22, no. 3, pp. 1032–1041, Mar. 2013.

[5] X. Wu, X. Liu, K. Hiramatsu, and K. Kashino, "Contrast-accumulated histogram equalization for image enhancement," in *Proc. IEEE Int. Conf. Image Process.*, Sep. 2017, pp. 3190–3194.

[6] P. Trahanias and A. Venetsanopoulos, "Color image enhancement through 3-D histogram equalization," in *Proc. IAPR Int. Conf. Pattern Recognit.*, Aug. 1992, pp. 545–548.
[7] D. Menotti, L. Najman, A. de A. Araujo, and J. Facon, "A fast hue-preserving histogram equalization method for color image enhancement using a Bayesian framework," in *Proc. 14th Int. Workshop Syst., Signals Image Process. 6th EURASIP Conf. Focused Speech Image Process., Multimedia Commun. Services*, Jun. 2007, pp. 414–417.
[8] J.-H. Han, S. Yang, and B.-U. Lee, "A novel 3-D color histogram equalization method with uniform 1-D gray scale histogram," *IEEE Trans. Image Process.*, vol. 20, no. 2, pp. 506–512, Feb. 2011.
[9] X. Fu, D. Zeng, Y. Huang, X.-P. Zhang, and X. Ding, "A weighted variational model for simultaneous reflectance and illumination estimation," in *Proc. IEEE Conf. Comput. Vis. Pattern Recognit.*, Jun. 2016, pp. 2782–2790.
[10] X. Guo, Y. Li, and H. Ling, "LIME: Low-light image enhancement via illumination map estimation," *IEEE Trans. Image Process.*, vol. 26, no. 2, pp. 982–993, Feb. 2017.
[11] Z. Ying, G. Li, and W. Gao, "A bio-inspired multi-exposure fusion framework for low-light image enhancement," *arXiv1711.00591*, Nov. 2017. [Online]. Available: http://arxiv.org/abs/1711.00591
[12] Y. Kinoshita and H. Kiya, "Automatic exposure compensation using an image segmentation method for single-image-based multi-exposure fusion," *APSIPA Trans. Signal Inf. Process.*, vol. 7, p. e22, Dec. 2018.
[13] M. Gharbi, J. Chen, J. T. Barron, S. W. Hasinoff, and F. Durand, "Deep bilateral learning for real-time image enhancement," *TOGACM Trans. Graph.*, vol. 36, no. 4, pp. 1–12, Jul. 2017.
[14] L. Shen, Z. Yue, F. Feng, Q. Chen, S. Liu, and J. Ma, "MSR-net: Low-light image enhancement using deep convolutional network," Nov. 2017, *arXiv1711.02488*. [Online]. Available: http://arxiv.org/abs/1711.02488
[15] J. Cai, S. Gu, and L. Zhang, "Learning a deep single image contrast enhancer from multi-exposure images," *IEEE Trans. Image Process.*, vol. 27, no. 4, pp. 2049–2062, Apr. 2018.
[16] C. Chen, Q. Chen, J. Xu, and V. Koltun, "Learning to see in the dark," in *Proc. IEEE Conf. Comput. Vis. Pattern Recognit.*, Jun. 2018, pp. 3291–3300.
[17] X. Yang, K. Xu, Y. Song, Q. Zhang, X. Wei, and R. W. Lau, "Image correction via deep reciprocating HDR transformation," in *Proc. IEEE Conf. Comput. Vis. Pattern Recognit.*, Jun. 2018, pp. 1798–1807.
[18] W. Ruixing, Q. Zhang, C.-W. Fu, X. Shen, W.-S. Zheng, and J. Jia, "Underexposed photo enhancement using deep illumination estimation," in *Proc. IEEE Conf. Comput. Vis. Pattern Recognit.*, Jun. 2019.
[19] Y. Kinoshita and H. Kiya, "Convolutional neural networks considering local and global features for image enhancement," in *Proc. IEEE Int. Conf. Image Process.*, Sep. 2019.
[20] S. Naik and C. Murthy, "Hue-preserving color image enhancement without gamut problem," *IEEE Trans. Image Process.*, vol. 12, no. 12, pp. 1591–1598, Dec. 2003.
[21] M. Nikolova and G. Steidl, "Fast hue and range preserving histogram specification: Theory and new algorithms for color image enhancement," *IEEE Trans. Image Process.*, vol. 23, no. 9, pp. 4087–4100, Sep. 2014.
[22] Y. Ueda, H. Misawa, T. Koga, N. Suetake, and E. Uchino, "HUE-preserving color contrast enhancement method without gamut problem by using histogram specification," in *Proc. IEEE Int. Conf. Image Process.*, Oct. 2018, pp. 1123–1127.
[23] T. Azetsu and N. Suetake, "Hue-preserving image enhancement in CIELAB color space considering color gamut," *Opt. Rev.*, vol. 26, no. 2, pp. 283–294, Apr. 2019.
[24] D. Jobson, Z. Rahman, and G. Woodell, "Properties and performance of a center/surround retinex," *IEEE Trans. Image Process.*, vol. 6, no. 3, pp. 451–462, Mar. 1997.
[25] D. Jobson, Z. Rahman, and G. Woodell, "A multiscale retinex for bridging the gap between color images and the human observation of scenes," *IEEE Trans. Image Process.*, vol. 6, no. 7, pp. 965–976, Jul. 1997.
[26] B. Cai, X. Xu, K. Guo, K. Jia, B. Hu, and D. Tao, "A joint intrinsic-extrinsic prior model for retinex," in *Proc. IEEE Int. Conf. Comput. Vis.*, Oct. 2017, pp. 4020–4029.
[27] E. H. Land, "The retinex theory of color vision," *Sci. Amer.*, vol. 237, no. 6, pp. 108–129, 1977.
[28] Y. Kinoshita and H. Kiya, "Scene segmentation-based luminance adjustment for multi-exposure image fusion," *IEEE Trans. Image Process.*, vol. 28, no. 8, pp. 4101–4116, Aug. 2019.
[29] K. Gu, G. Zhai, X. Yang, W. Zhang, and C. W. Chen, "Automatic contrast enhancement technology with saliency preservation," *IEEE Trans. Circuits Syst. Video Technol.*, vol. 25, no. 9, pp. 1480–1494, Sep. 2015.
[30] K. Gu, G. Zhai, W. Lin, and M. Liu, "The analysis of image contrast: From quality assessment to automatic enhancement," *IEEE Trans. Cybern.*, vol. 46, no. 1, pp. 284–297, Jan. 2016.
[31] K. Gu, D. Tao, J.-F. Qiao, and W. Lin, "Learning a no-reference quality assessment model of enhanced images with big data," *IEEE Trans. Neural Netw. Learn. Syst.*, vol. 29, no. 4, pp. 1301–1313, Apr. 2018.
[32] K. Dabov, A. Foi, V. Katkovnik, and K. Egiazarian, "Color image denoising via sparse 3D collaborative filtering with grouping constraint in luminance-chrominance space," in *Proc. IEEE Int. Conf. Image Process.*, Sep. 2007, pp. 313–316.
[33] H. Kobayashi and H. Kiya, "JPEG XT image compression with hue compensation for two-layer HDR coding," in *Proc. IEEE Int. Conf. Consum. Electron.-Asia*, Jun. 2019.
[34] Y. Kinoshita and H. Kiya, "iTM-net: Deep inverse tone mapping using novel loss function considering tone mapping operator," *IEEE Access*, vol. 7, pp. 73555–73563, 2019.
[35] *HDR Photography Gallery*. Accessed: Mar. 2019. [Online]. Available: https://www.easyhdr.com/examples/
[36] D. Kundu, D. Ghadiyaram, A. C. Bovik, and B. L. Evans, "No-reference quality assessment of tone-mapped HDR pictures," *IEEE Trans. Image Process.*, vol. 26, no. 6, pp. 2957–2971, Jun. 2017.
[37] K. Gu, W. Lin, G. Zhai, X. Yang, W. Zhang, and C. W. Chen, "No-reference quality metric of contrast-distorted images based on information maximization," *IEEE Trans. Cybern.*, vol. 47, no. 12, pp. 4559–4565, Dec. 2017.
[38] *Colorimetry-Part 6: CIEDE2000 Colour-Difference Formula*, Standard ISO/CIE 11664-6:2014, ISO/CIE, 2014.
[39] V. Bychkovsky, S. Paris, E. Chan, and F. Durand, "Learning photographic global tonal adjustment with a database of input/output image pairs," in *Proc. IEEE Conf. Comput. Vis. Pattern Recognit.*, Jun. 2011, pp. 97–104.

YUMA KINOSHITA (Student Member, IEEE) received the B.Eng. and M.Eng. degrees from Tokyo Metropolitan University, Japan, in 2016 and 2018, respectively, where he is currently pursuing the Ph.D. degree. His research interest is in the area of image processing. He is a Student Member of APSIPA and IEICE. He received the IEEE ISPACS Best Paper Award, in 2016, the IEEE Signal Processing Society Japan Student Conference Paper Award, in 2018, the IEEE Signal Processing Society Tokyo Joint Chapter Student Award, in 2018, and the IEEE GCCE Excellent Paper Award (Gold Prize), in 2019.

HITOSHI KIYA (Fellow, IEEE) received the B.E. and M.E. degrees from the Nagaoka University of Technology, in 1980 and 1982, respectively, and the Dr.Eng. degree from Tokyo Metropolitan University, in 1987. In 1982, he joined Tokyo Metropolitan University, where he became a Full Professor, in 2000. From 1995 to 1996, he was a Visiting Fellow with The University of Sydney, Sydney, NSW, Australia. He served as the Inaugural Vice President (Technical Activities) of APSIPA, from 2009 to 2013, and the Regional Director-at-Large for Region ten of the IEEE Signal Processing Society, from 2016 to 2017. He was also the President of the IEICE Engineering Sciences Society, from 2011 to 2012. He currently serves as the President of APSIPA. He is a Fellow of IEICE and ITE. He served as the Vice President and the Editor-in-Chief for IEICE Society Magazine and Society Publications. He was a recipient of numerous awards, including nine best paper awards. He was the Chair of two technical committees and a member of nine technical committees, including the APSIPA Image, Video, and Multimedia Technical Committee (TC) and the IEEE Information Forensics and Security TC. He has organized a lot of international conferences in such roles as the TPC Chair of the IEEE ICASSP 2012 and the General Co-Chair of the IEEE ISCAS 2019. He was an Editorial Board Member of eight journals, including the IEEE TRANSACTIONS ON SIGNAL PROCESSING, *Image Processing*, and *Information Forensics and Security*.